An ionic liquid incorporated gel polymer electrolyte for double layer capacitors

Kumudu S. Perera[*], K.W. Prasadini and Kamal P. Vidanapathirana

Polymer Electronics Research Group. Department of Electronics,
Wayamba University of Sri Lanka, Kuliyapitiya, Sri Lanka

Abstract. Energy storage devices have received a keen interest throughout the world due to high power consumption. A large number of research activities are being conducted on electrochemical double layer capacitors (EDLCs) because of their high power density and higher energy density. In the present study, an EDLC was fabricated using natural graphite based electrodes and ionic liquid (IL) based gel polymer electrolyte (GPE). The IL based GPE was prepared using the IL, 1-ethyl-3-methylimidazolium trifluoromethanesulfonate (1E3MITF) with the polymer poly(vinyl chloride) (PVC) and the salt magnesium trifluoromethanesulfonate ($Mg(CF_3SO_3)_2$ - MgTF). GPE was characterized by electrochemical impedance spectroscopy (EIS), DC polarization test, linear sweep voltammetry (LSV) test and cyclic voltammetry (CV) test. The maximum room temperature conductivity of the sample was 1.64×10^{-4} Scm^{-1}. The electrolyte was purely an ionic conductor and the anionic contribution was prominent. Fabricated EDLC was characterized by EIS, CV and galvanostatic charge discharge (GCD) tests. CV test of the EDLC exhibits a single electrode specific capacitance of 1.44 Fg^{-1} initially and GCD test gives 0.83 Fg^{-1} as initial single electrode specific discharge capacitance. Moreover, a good stability was observed for prolonged cycling and the device can be used for applications with further modifications.

Keywords: ionic liquid; electrochemical double layer capacitor; natural graphite; gel polymer electrolyte; 1-ethyl-3-methylimidazolium trifluoromethanesulfonate

1. Introduction

Electrochemical double layer capacitors (EDLCs) have been recognized as attractive energy storage devices by researchers due to their high power densities and high energy densities compare to batteries and conventional capacitors (Kang *et al*. 2014). In EDLCs, there are no faradic reactions involved. Instead, the operation is based on the reversible adsorption of ions between the electrodes and the electrolyte. EDLCs are fabricated with carbon-based electrodes such as activated carbon, single-walled and multi-walled carbon nanotubes (Pandey *et al.* 2010a).

High power performance of EDLC can be achieved by the use of high conducting aqueous electrolytes. However, due to the narrow electrochemical stability window of water, these EDLCs

---

*Corresponding author, Professor, E-mail: kumudu31966@gmail.com

show narrow operating voltages (Syahidah and Majid 2015). In this context, gel polymer electrolytes (GPEs) have received an intense interest due to their high conductivities at room temperature, good mechanical properties and wider voltage window (Tafur *et al.* 2015). At present, it has been found that the presence of hazardous solvents in GPEs makes the path for poor reliability and safety issues. This has led to search novel methodologies to overcome such problems. One of the approaches is employing ionic liquids (ILs) which are room temperature molten salts possessing good conductivities, large liquid phase range, non-toxicity, non-flammability as well as stability (Kumar *et al.* 2011). They have been identified as viable and emerging class of substitutes for solvents.

ILs based GPES have been investigated using various polymer hosts including poly(vinylidene fluoride) (PVdF), poly(vinyl chloride) (PVC), poly(acrylonitrile) (PAN), poly(methyl methacrylate) (PMMA) (Rajendran *et al.* 2008, Bai *et al.* 2017).

Research activities on IL based GPEs have been intensively focused on lithium salt systems due to their attractive features. However, as those systems suffer various safety problems, attention has been focused on non Li materials like Mg, Zn and Na (Kumar *et al.* 2011).

In this study, an EDLC was fabricated using an IL based GPE comprising 1-ethyl-3-methylimidazolium trifluoromethanesulfonate (1E3MITF) as the IL, magnesium trifluoromethanesulfonate ($Mg(CF_3SO_3)_2$ - MgTF) as the salt and PVC as the polymer host. Optimum composition of the IL based GPE was found by the room temperature conductivity values obtaining from varying the IL composition. For characterization of optimized composition, DC polarization test, cyclic voltammetry (CV) test and linear sweep voltammetry tests were done. Moreover, to characterize the fabricated EDLC, electrochemical impedance spectroscopy (EIS), CV test and galvanostatic charge discharge (GCD) test were done at room temperature.

2. Experimental

2.1 Materials

Poly(vinyl chloride) (PVC, high molecular weight), 1-ethyl-3-methylimidazolium trifluoromethanesulfonate (1E3MITF, 98%), tetrahydrofuran (THF) were obtained from Sigma-Aldrich and were used as received. Magnesium trifluoromethanesulfnate ($Mg(CF_3SO_3)_2$ - MgTF) was obtained from Sigma-Aldrich and dried at 100°C for 1 hour to eliminate the trace amounts of water prior to the preparation of the gel polymer electrolyte (GPE).

2.2 Preparation of the gel polymer electrolyte (GPE)

GPE was prepared using traditional solvent casting technique. First, PVC was dissolved in THF and well stirred using a magnetic stirrer. After PVC was completely dissolved, required amounts of MgTF and 1E3MITF were added and stirred again until a homogeneous solution was obtained. The resulting mixture was poured into a glass petri dish and allowed for evaporation of THF overnight. Finally, it was possible to observe a thin, bubble free film. GPE films were prepared by varying the composition of 1E3MITF. Optimized composition was determined using the highest ionic conductivity value.

2.3 Characterization of GPE

2.3.1 AC conductivity measurements

Circular shaped samples were cut from resulted GPE film and it was sandwiched in between two well cleaned stainless steel (SS) discs. Impedance data were collected in the frequency range of 0.1 Hz to 400 kHz and the temperature range from 28℃ to 55℃ using a Metrohm Autolab M101 impedance analyzer for all prepared samples.

2.3.2 DC polarization test

A circular shaped sample was loaded inside a Teflon sample holder first between two SS (blocking) electrodes and then between two Mg (non-blocking) electrodes. Current variation with time was observed under 1.0 V DC potential with SS electrodes and under 0.5 V DC potential with Mg electrodes. Both tests were performed at room temperature.

2.3.3 Linear and cyclic voltammetry studies

The GPE which has the maximum conductivity value was selected for linear and cyclic voltammetry (CV) tests. The GPE film was sandwiched in between SS and Mg electrodes and assembled in a spring loaded sample holder. Linear sweep voltammetry study was performed in the potential range of -2.0 V-6.0 V at the scan rate of 5 mVs⁻¹. A computer controlled Metrohm Autolab potentiostat M101 was used to obtain the current variation with potential. Using the same instrument, CV measurements were taken within the potential window of -2.8 V to 2.8 V at the scan rate of 10 mVs⁻¹ for cells in the configurations, SS / GPE / SS and Mg / GPE / Mg in order to observe the plating/stripping effect of Mg ions.

2.4 Preparation of electrode and fabrication of the EDLC

Poly(vinylidene fluoride) (PVdF) was dissolved in acetone by magnetic stirring. Pre heated natural graphite was well mixed with PVdF into required ratio. The resulted mixture was then thoroughly stirred with Athena-Ultrasonic homogenizer to obtain a well-mixed slurry. Then, the slurry was evenly coated on the fluorine-doped tin oxide (FTO) glass strips.

Ionic liquid (IL) based GPE was sandwiched in between two identical graphite electrodes for the purpose of fabrication of the EDLC. Area of a single electrode of the EDLC was 1 cm².

2.5 Performance evaluation of the EDLC

2.5.1 Electrochemical impedance spectroscopy (EIS)

Impedance measurements of the EDLC were gathered in the frequency range from 0.005 Hz to 400 kHz at room temperature using Metrohm Autolab potentiostat M101. Nyquist plots and bode plots were drawn to observe capacitive effect as well as to calculate the relaxation time.

2.5.2 Cyclic voltammetry (CV) analysis

CV tests were carried out using a three-electrode cell having one graphite electrode as the working electrode and the other graphite electrode as the reference and counter electrode. Scanning was done within various potential windows and at various scan rates. Then, the continuous cycling was done within the potential window and at the scan rate that results the optimum performance.

2.5.3 Galvanostatic charge discharge (GCD) test

The galvanostatic charge discharge (GCD) test of the EDLC was performed in between the potentials 0.1 V and 2.0 V under a constant current of 2.4 x 10⁻⁵ A for 1000 cycles.

3. Results and discussion

3.1 Characterization of GPE

3.1.1 Electrochemical impedance spectroscopy (EIS)

Electrochemical impedance spectroscopy is a powerful tool that is available for demonstrating several electrical properties of materials as well as various electrochemical devices. Fig.1 displays the resulted nyquist plot of an IL based GPE at room temperature.

The ionic conductivity (σ) was calculated using impedance data obtained from EIS via the equation,

$$\sigma = (1/R_b)(l/A) \tag{1}$$

where l is the thickness of the electrolyte, A is the surface area of the electrolyte and R_b is the bulk electrolyte resistance (Ramesh *et al.* 2013).

In Nyquist plot, x axis is taken as the real axis and y axis as the imaginary axis. In general, Nyquist plot of a symmetrical SS/ GPE/ SS cell configuration consists of two semi circles at high and middle frequency regions and one spike at low frequency region. High frequency semi-circle corresponds to bulk electrolyte resistance (R_b) whereas middle frequency semi-circle corresponds to charge transfer resistance (R_{ct}) at the interfaces. Spike at low frequency stands for diffusion controlled capacitive features (Song *et al.* 2003). In the present study high frequency semi-circle was absent because of the unavailability of high frequency values. The first intercept of the existing semi-circle was used to calculate R_b of the electrolytes.

Room temperature conductivity (σ_{RT}) variation with different IL compositions based on weight ratio is shown in Fig. 2.

According to the figure, a gradual increase of room temperature conductivity can be observed with the increase of IL concentration. After achieved the maximum conductivity of 1.64 x 10^{-4} Scm^{-1} at PVC (1) : MgTF (2) : IL (1.75) composition, there is a decrease in the ionic conductivity
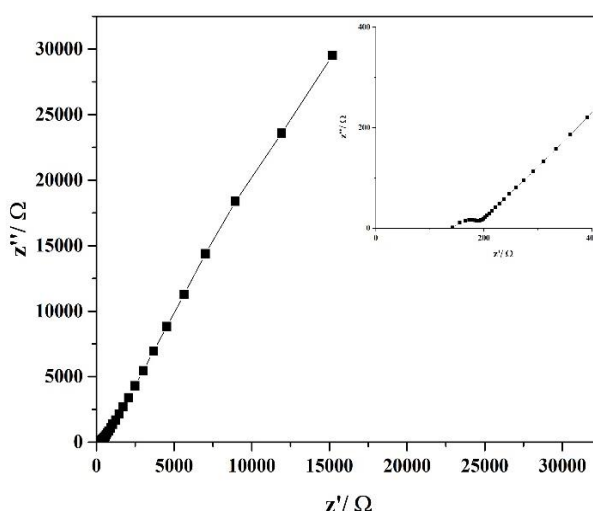

Fig. 1 Resulted Nyquist plot of an IL based GPE at room temperature within the frequency range 0.1 Hz to 400 kHz
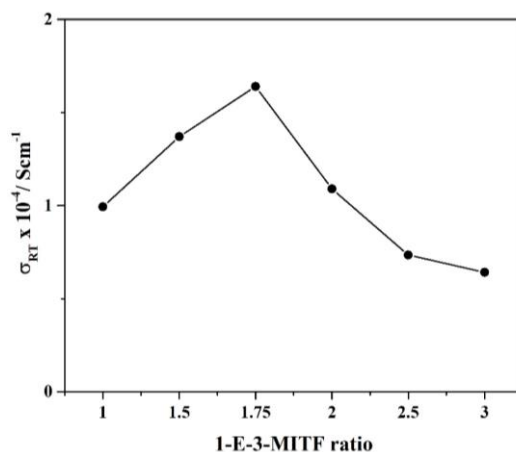
Fig. 2 Room temperature conductivity (σ_{RT}) variation with different IL composition (weight ratio)
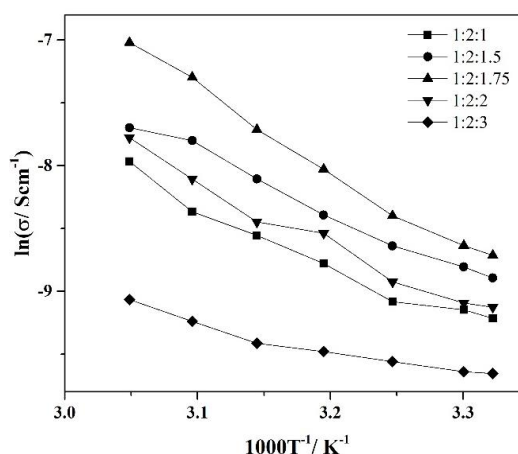

Fig. 3 Temperature dependence conductivity for various IL compositions

on further addition of IL. It is a well-known fact that the conductivity depends on charge carrier concentration as well as mobility of charge carriers. The possible reason for the improvement of ionic conductivity can be generation of ions such as $1E3MI^+$ and $CF_3SO_3^-$ upon increasing the concentration of IL (Bandara *et al*. 2013). Moreover, the decrease of conductivity after IL ratio of 1.75 may be due to the association effect, which forms ion pairs, triplets and aggregates that are not supporting the ionic conductivity (Kumar *et al*. 2011). While increasing the IL concentration, there is a possibility of increase of viscosity of the medium disturbing charge carrier motion very much. This may also reduce conductivity of the system.

Fig. 3 illustrates the variation of the natural logarithm of the conductivity with inverse temperature at different IL concentrations.

When increasing the temperature, conductivity is also increasing. The possible reason can be due to increasing the mobility of ions when they get energized with increasing temperature. Conductivity of all compositions show a near linear behavior with temperature. This suggests that all compositions obey Arrhenius behavior which showcases the fact that the conductivity takes
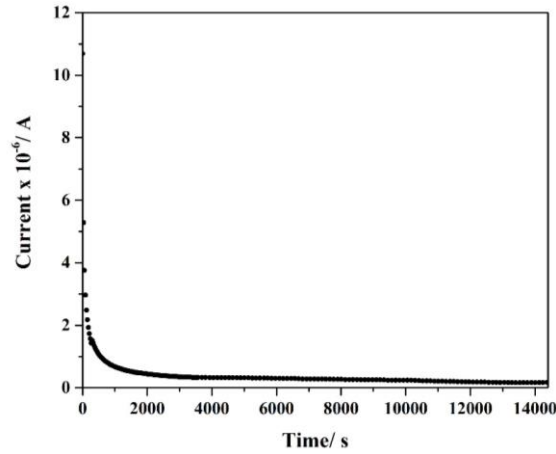
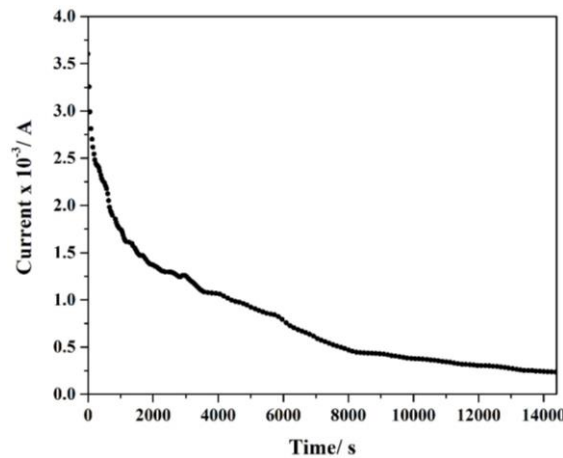Fig. 4 Current variation with time for the configuration SS/GPE/SS under 1 V DC potential

Fig. 5 Current variation with time for Mg / GPE / Mg cell under 0.5 V DC potential

place via hopping mechanism. Arrhenius equation can be given by

$$\sigma(T) = A\, exp(-E_a / k_B\, T) \qquad (2)$$

where A is the pre-exponential factor, E_a is the activation energy, T is the absolute temperature and k_B is the Boltzmann constant (Arof *et al.* 2014).

3.1.2 DC polarization test

Current variation with time for the configuration, SS / GPE / SS is shown in Fig. 4. The initial current dropped very quickly and then, the steady state current reached. Initially, ions tend to polarize and then a large current can be obtained. The ionic motion is blocked with time and as a result, current decreased rapidly. Finally, only electron movement remains giving rise to a constant current.

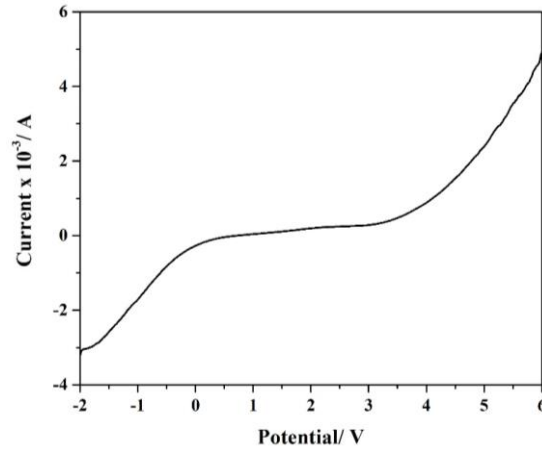Ionic transference number, t_i was calculated using the equation,

Fig. 6 Linear sweep voltammogram for the configuration SS / GPE / Mg at the scan rate of 5 mVs⁻¹
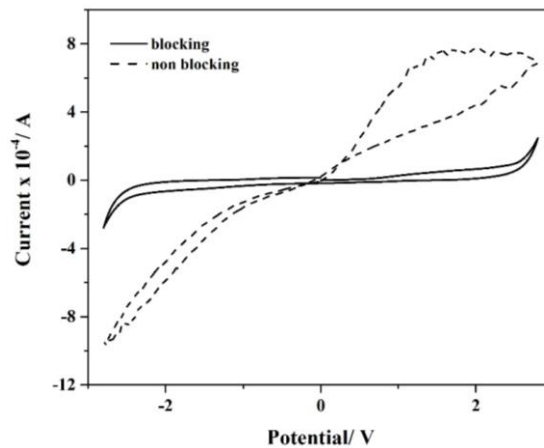

Fig. 7 Cyclic voltammogrammes of configurations, SS / GPE / SS and Mg / GPE / Mg at the scan rate of 10 mVs⁻¹

$$t_{ion} = (I_i - I_0) / I_i \qquad (3)$$

where I_i is the initial current, and I_0 is the stable current. In the present study, all t_i values were higher than 0.97. These higher values indicate that the major charge carrier of GPE samples are ions (Rosdi *et al*. 2016).

Current variation with time under a DC potential of 0.5 V for the configuration Mg/GPE/Mg is shown in Fig. 5. The cationic transference number (t_{cation}) was calculated using the following equation

$$t_{cation} = I_{cation} / I_{total} \qquad (4)$$

where I_{total} is the total current due to anions and cations and I_{cation} is the current due to cations (Kumar and Sampath 2003).

According to Fig. 5, the initial drop of current is very high. This is due to the movement of anions which are blocked by Mg electrodes. The steady state current followed by the drop is due to cations. The calculated value for cationic transference number was 0.09. In other words, anionic transference number was 0.91. This indicates that the effect of anionic charge ($CF_3SO_3^-$) on the conductivity is dominant in the electrolyte (Kumar and Hashmi 2010).

3.1.3 Linear and cyclic voltammetry studies

The electrochemical stability window of a GPE can be evaluated by LSV. The resulted linear sweep voltammogram for the cell SS / GPE / Mg obtained at the scan rate of 5 mVs^{-1} and within the potential window -2.0 V to 6.0 V is shown in Fig. 6. The voltage stability window can be observed between 0.5 V to 3.0 V. This result suggests that the fabricated IL based GPE is suitable for practical applications.

The cyclic voltammograms within the potential window -2.8 V to 2.8 V for the configurations SS / GPE / SS and Mg / GPE / Mg are shown in Fig. 7.

It is obvious that there are no peaks in SS / GPE / SS configuration. However, small peaks are present in Mg / GPE / Mg configuration. This reveals platting and stripping of Mg is possible only on Mg electrodes but not on the SS electrodes (Osman *et al*. 2012).

3.2 Characterization of EDLC

3.2.1 Electrochemical impedance spectroscopy (EIS)

Fig. 8 shows resulted Nyquist plot for the fabricated EDLC.

Generally, Nyquist plot of an EDLC consists of a semi-circle at high frequencies, which represents bulk electrolyte resistance (Mei *et al*. 2018). Spikes having two inclinations can be seen at low frequency region representing the diffusion and capacitive behavior. Among them, the lowest frequency region spike becomes parallel to the imaginary impedance axis (Y-axis) confirming pure capacitive behavior (An *et al*. 2001).
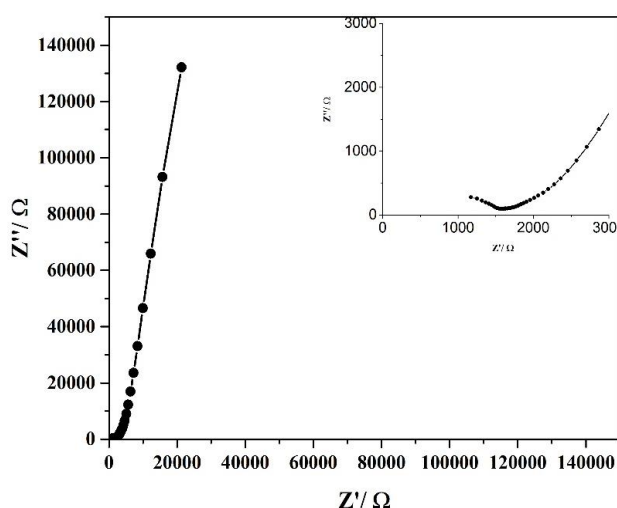

Fig. 8 Nyquist plot of EDLC with natural graphite and PVdF cathode at 0.005 Hz to 400 kHz

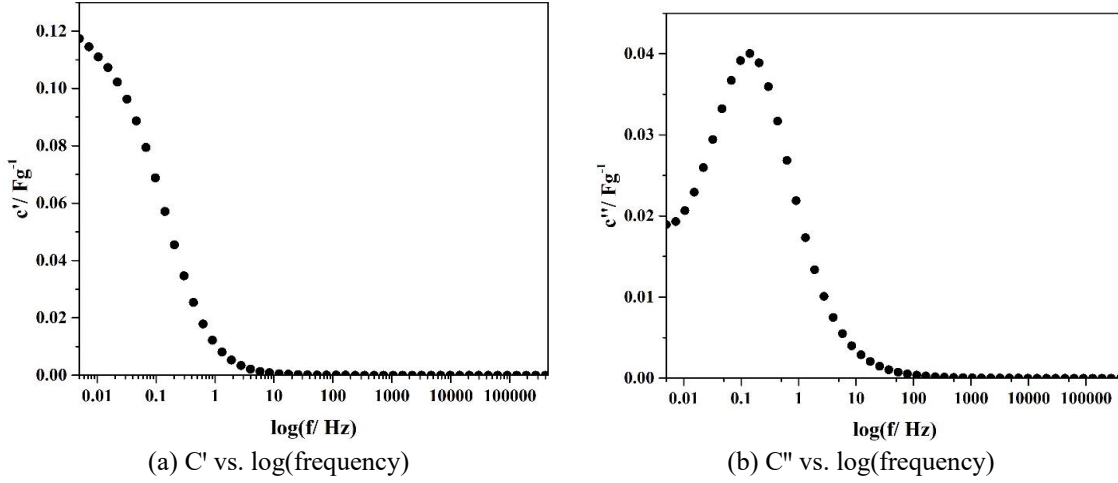(a) C' vs. log(frequency) (b) C" vs. log(frequency)

Fig. 9 Bode plots from 0.005 Hz to 400 kHz frequency range of EDLC

In the resulting Nyquist plot (Fig .8), the high frequency semi-circle was not present. This may be because of the unavailability of required high frequency values. A non-vertical line at mid frequency range is having about 45° inclination and it represents the diffusion called Warburg diffusion. The resulting line at low frequency range is not perfectly parallel to the imaginary (z") axis. The reason for not observing a vertical line may be due to the surface roughness as well as non-uniform active layer thickness (Prabaharan *et al.* 2006).

Fig. 9(a) and 9(b) represent the variation of real and imaginary capacitances with logarithmic scale of frequency. The capacitance is a complex term and can be given in terms of frequency as follows.

$$C(\omega) = C'(\omega) + jC''(\omega) \qquad (5)$$

where $C'(\omega)$ is the real part of complex capacitance and $C''(\omega)$ is the imaginary part of the complex capacitance.

$C'(\omega)$ and $C''(\omega)$ were calculated based on the real, $(Z'(\omega))$ and imaginary $(Z''(\omega))$ parts of the impedance as follows.

$$C'(\omega) = -Z''(\omega) \div [\,|\omega| Z(\omega)^2\,] \qquad (6)$$

$$C''(\omega) = Z'(\omega) \div [\,|\omega| Z(\omega)^2\,] \qquad (7)$$

where Z is the complex impedance (Tey *et al.* 2016).

The fabricated EDLC shows a maximum C' of 0.18 Fg^{-1}. In addition, the relaxation time (τ_0) which is a quantitative measurement of the reversible charge discharge rate of the EDLC was calclated as,

$$\tau_0 = 1/2\pi f_0 \qquad (8)$$

where f_0 is the frequency at maximum C''. Calculated relaxation time of the fabricated EDLC was 1.09 s. This indicates ion transfer is fairly fast (Voigt and Wulle 2012).

3.2.2 Cyclic voltammetry tests

Fig. 10 shows the cyclic voltammogrammes obtained for the EDLC varyig the potential window at the scan rate of 10 mVs⁻¹.

According to the resulted cyclic voltammograms there were no distinct peaks obtained in all windows due to no redox reactions were taking place at the graphite based electrodes of EDLC. It involves accumulation of charges at the electrode/electrolyte interface and within the electrode (Gao *et al*. 2014). When the width of the potential window was increased beyond 2.0 V, current increased very much and the symmetry of the current response about the zero current line is destroyed. This can be because of the unwanted reactions at wider windows which may cause degradation of EDLC (Harankahawa *et al*. 2017). For further experiments 0.1 V to 2.0 V was taken as the optimized window.
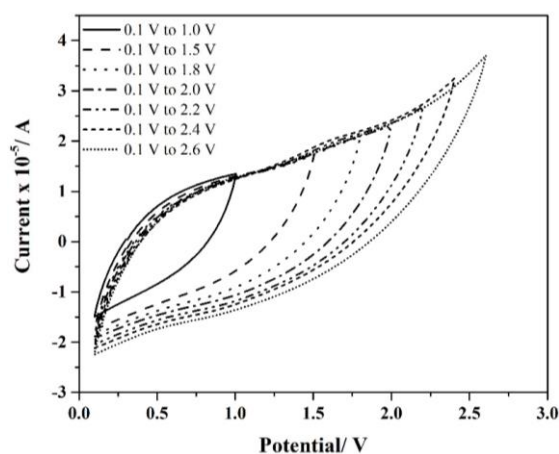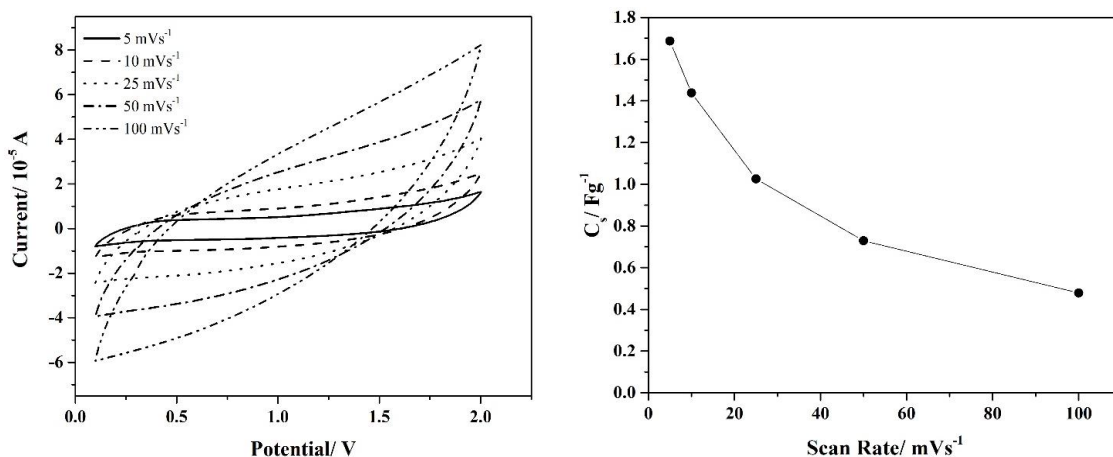

Fig. 10 Cyclic voltammograms obtained at the scan rate of 10 mVs⁻¹ within different potential windows

(a) Cyclic voltammograms obtained at different scan rates within the potential window of 0.1 V to 2.0 V

(b) Variation of single electrode specific capacitance with different scan rates within the potential window of 0.1 V to 2.0 V

Fig. 11 Cyclic voltammogrammes for different scan rates and variation of single electrode specific capacitance with the scan rate

Cyclic voltammograms for different scan rates and their single electrode specific capacitance values (C_s) are shown in Fig. 11. Specific capacitance was calculated as

$$Cs = 2 \int I \, dv \, / \, (m \, S \, \Delta v) \tag{9}$$

where, $\int Idv$ is the area under the cyclic voltammograms, m is the mass of an electrode, S is the scan rate and ΔV is the width of the potential window (Wang *et al.* 2013).

There were no visible peaks in the cyclic voltammogrammes due to the absence of redox reactions. All cyclic voltammograms at different scan rates are near mirror images around zero current axis and show rectangular shapes. This indicates the capacitive behaviour of the EDLC due to the formation of a double layer (Pandey *et al.* 2010b). Moreover, at higher scan rates, the current value increased which may lead to some destructive reactions of the EDLC. When increasing the scan rate, single electrode specific capacitance decreased. The reason for this is insufficient time left for the reactions to take place completely (Bandaranayake *et al.* 2015).
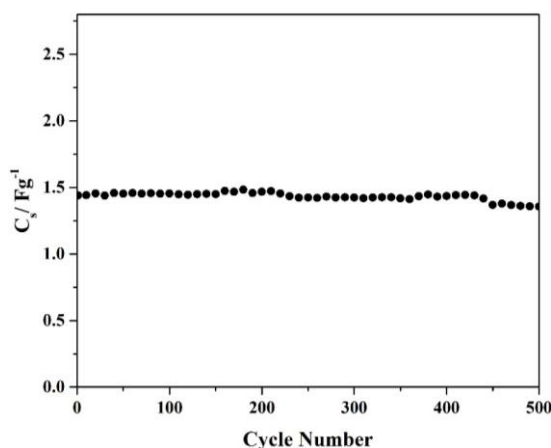

Fig. 12 Single electrode specific capacitance variation with the cycle number at the scan rate of 10 mVs^{-1} and within the potential window of 0.1 V to 2.0 V
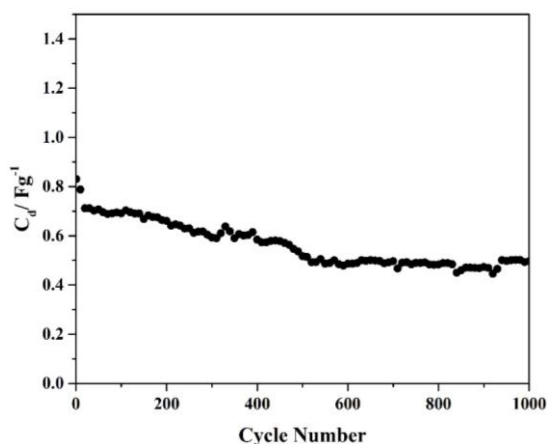

Fig. 13 Single electrode discharge capacitance variation for 1000 galvanostatic charge discharge cycles

Fig. 12 illustrates the variation of the single electrode specific capacitance (C_s) for 500 cyclic voltammograms.

Cycling life of a EDLC is one of the important parameters for practical applications. Initial single electrode specific capacitance of the fabricated EDLC was 1.44 Fg^{-1}. After 500 cycles it was 1.36 Fg^{-1}. The retention of the single electrode specific capacitance is about 5.85% over 500 cycles. This is an indication for the stability among electrode/electrolyte components.

3.2.3 Galvanostatic charge discharge test

Single electrode specific discharge capacitance (C_d) can be calculated from the GCD test using the equation,

$$C_d = I\, dt\, /\, (m\, dV) \tag{10}$$

where *I* is the constant current, m is the mass of a single electrode, dV/ dt is the rate of drop of potential excluding IR drop during discharge (Pandey and Rastogi 2012)

Variation of the single electrode specific discharge capacitance, C_d is plotted with the galvanostatic charge discharge cycles in Fig. 13.

Initial single electrode discharge capacitance of EDLC was 0.83 Fg^{-1}. According to the figure, there are up and down variations in the single electrode discharge capacitance. This may due to some oxidation reactions which are reversible. Maintaining such variations without disturbing the performance of EDLC reveals the 'self healing property' of GPE (Cheng *et al*. 2017). It is obvious that the single electrode discharge capacitance is decreasing over 1000 cycles. Decrease of C_d value can be due to loss of interfacial contacts between the electrode and electrolyte and also due to degradation of electrolyte and/or electrodes.

4. Conclusions

1E3MITF based GPE was successfully fabricated by solvent casting technique. The maximum room temperature conductivity was 1.64 x 10^{-4} Scm^{-1} and the respective composition was PVC (1) : MgTF (2) : IL (1.75). Conductivity of all fabricated IL based GPEs take place via hopping mechanism. The electrolyte was purely an ionic conductor and the contribution from anionic charge on conductivity is prominent according to transference number measurements. It shows that the electrochemical stability window lies between 0.5 V and 3.0 V. Mg plating and stripping takes place on the Mg electrodes but not on SS electrodes. The fabricated EDLC with Sri Lankan natural graphite and PVdF host polymer shows relaxation time of 1.09 s. The continuous cyclic voltammograms were performed in between 0.1 V to 2.0 V potential window and the scan rate of 10 mVs^{-1}. The initial single electrode specific capacitance from continuous CV measurements was 1.44 Fg^{-1}. The efficiency of the single electrode specific capacitance remained at 94.15% over 500 cycles. Continuous charging discharging cycles results a single electrode specific discharge capacitance of 0.83 Fg^{-1} at the first cycle and it gradually decreased with continuous cycling. Moreover, the EDLC has a good stability. This device can be used as an energy storage device with further modifications.

Acknowledgments

References

An, K.H., Kim, W.S., Park, Y.S., Moon, J.M., Bae, D.J., Lim, S.C., Lee, Y.S. and Lee, Y.H. (2001), "Electrochemical properties of high-power supercapacitors using single-walled carbon nanotube electrodes", *Adv. Funt. Mater.*, **11**(5), 387-392. https://doi.org/10.1002/1616-3028(200110)11:5%3C387::AID-ADFM387%3E3.0.CO;2-G.

Arof, A.K., Aziz, M.F., Noor, M.M., Careem, M.A., Bandara, L.R.A.K., Thotawatthage, C.A., Rupasinghe, W.N.S. and Dissanayake, M.A.K.L. (2014), "Efficiency enhancement by mixed cation effect in dye-sensitized solar cells with a PVdF based gel polymer electrolyte", *Int. J. Hydrogen Energy*, **39**, 2929-2935. https://doi.org/10.1016/j.ijhydene.2013.07.028.

Bai, J., Lu, H., Cao, Y., Li, X. and Wang, J. (2017), "A novel ionic liquid polymer electrolyte for quasi-solid state lithium air batteries", *RSC Adv.*, **7**(49), 30603-30609. https://doi.org/10.1039/C7RA05035F.

Bandara, T.M.W.J., Svensson, T., Dissanayake, M.A.K.L., Furlani, M., Jayasundara, W.J.M.J.S.R., Fernando, P.S.L., Albinsson, I. and Mellander, B.E. (2013), "Conductivity behaviour in novel quasi-solid-state electrolyte based on polyacrylonitrile and tetrahexylammonium iodide intended for dye sensitized solar cells", *J. Natl. Sci. Found. Sri Lanka*, **41**(3), 175-184. https://doi.org/10.4038/jnsfsr.v41i3.6056.

Bandaranayake, C.M., Jayathilake, Y.M.C.D., Vidanapathirana, K.P. and Perera, K.S. (2015), "Performance of a sodium thiocyanate based gel polymer electrolyte in redox capacitors", *Sabaragamuwa Univ. J.*, **14**(2), 149-161. https://doi.org/10.4038/suslj.vI4i2.7702.

Cheng, X., Pan, J., Zhao, Y., Liao, M. and Peng, H. (2018), "Gel polymer electrolytes for electrochemical energy storage", *Adv. Energy Mater.*, **8**(7), 1-16. https://doi.org/10.1002/aenm.201702184.

Gao, Z., Wang, F., Chang, J., Wu, D., Wang, X., Wang, X., Xu, F., Gao, S. and Jiang, K. (2014), "Chemically grafted graphene-polyaniline composite for application in supercapacitor", *Electrochim. Acta*, **133**, 325-334. https://doi.org/10.1016/j.electacta.2014.04.033.

Harankahawa, N.S., Weerasinghe, S., Vidanapathirana, K. and Perera, K. (2017), "nvestigation of a pseudo capacitor with polyacrylonitrile based gel polymer electrolyte", *J. Electrochem. Sci. Technol.*, **8**(2), 107-114. https://doi.org/10.5229/JECST.2017.8.2.107.

Kang, J., Wen, J., Jayaram, S.H., Yu, A. and Wang, X. (2014), "Development of an equivalent circuit model for electrochemical double layer capacitors (EDLCs) with distinct electrolytes", *Electrochim. Acta*, **115**, 587-598. https://doi.org/10.1016/j.electacta.2013.11.002.

Kumar, D. and Hashmi, S.A. (2010), "Ionic liquid based sodium ion conducting gel polymer electrolytes", *Solid State Ionics*, **181**(8-10), 416-423. https://doi.org/10.1016/j.ssi.2010.01.025.

Kumar, G.G. and Sampath, S. (2003), "Electrochemical characterization of poly(vinylidenefluoride)-zinc triflate gel polymer electrolyte and its application in solid-state zinc batteries", *Solid State Ionics*, **160**(3-4), 289-300. https://doi.org/10.1016/s0167-2738(03)00209-1.

Kumar, Y., Hashmi, S.A. and Pandey, G.P. (2011), "Ionic liquid mediated magnesium ion conduction in poly(ethylene oxide) based polymer electrolyte", *Electrochim. Acta*, **56**(11), 3864-3873. https://doi.org/10.1016/j.electacta.2011.02.035.

Mei, B.A., Munteshari, O., Lau, J., Dunn, B. and Pilon, L. (2018), "Physical interpretations of Nyquist plots for EDLC electrodes and devices", *J. Phys. Chem. C*, **122**(1), 194-206. https://doi.org/10.1021/acs.jpcc.7b10582.

Osman, Z., Samin, S.M., Othman, L. and Isa, K.B.M. (2012), "Ionic transport in PMMA-NaCF$_3$SO$_3$ gel polymer electrolyte", *Adv. Mater. Res.*, **545**, 259-263. https://doi.org/10.4028/www.scientific.net/AMR.545.259.

Pandey, G.P. and Rastogi, A.C. (2012), "Pulse polymerized poly(3,4- Ethylene Dioxythiophene) electrodes for solid-state supercapacitors with ionic liquid gel polymer electrolyte", *Mater. Res. Soc. Symp. Proc.*, **1448**, 13-18. https://doi.org/10.1149/2.047210jes.

Pandey, G.P., Hashmi, S.A. and Kumar, Y. (2010a), "Performance studies of activated charcoal based electrical double layer capacitors with ionic liquid gel polymer electrolytes", *Energy Fuel*, **24**(12), 6644-6652. https://doi.org/10.1021/ef1010447.

Pandey, G.P., Kumar, Y. and Hashmi, S.A. (2010b), "Ionic liquid incorporated polymer electrolytes for supercapacitor application", *Indian J. Chem. Sect. A Inorganic Phys. Theor. Anal. Chem.*, **49,** 743-751.

Prabaharan, S.R.S., Vimala, R. and Zainal, Z. (2006), "Nanostructured mesoporous carbon as electrodes for supercapacitors", *J. Power Source.*, **161**(1), 730-736. https://doi.org/10.1016/j.jpowsour.2006.03.074.

Rajendran, S., Prabhu, M.R. and Rani, M.U. (2008), "Ionic conduction in poly(vinyl chloride)/poly(ethyl methacrylate)-based polymer blend electrolytes complexed with different lithium salts", *J. Power Source.*, **180**(2), 880-883. https://doi.org/10.1016/j.jpowsour.2008.02.063.

Ramesh, S., Lu, S.C. and Vankelecom, I. (2013), "BMIMTf ionic liquid-assisted ionic dissociation of MgTf in P(VdF-HFP)-based solid polymer electrolytes", *J. Phys. Chem. Solids*, **74**(10), 1380-1386. https://doi.org/10.1016/j.jpcs.2013.04.017.

Rosdi, A., Zainol, N.H. and Osman, Z. (2016), "Ionic transport and electrochemical stability of PVDF-HFP based gel polymer electrolytes", *AIP Conf. Proc.*, **1711**(1), 0500031-0500036. https://doi.org/10.1063/1.4941629.

Song, M.K., Kim, Y.T., Cho, B.W., Popov, B.N. and Rhee, H.W. (2003), "Thermally stable gel polymer electrolytes", *J. Electrochem. Soc.*, **150**(4), A439-A444. https://doi.org/10.1149/1.1556592.

Syahidah, S.N. and Majid, S.R. (2015), "Ionic liquid-based polymer gel electrolytes for symmetrical solid-state electrical double layer capacitor operated at different operating voltages", *Electrochim. Acta*, **175**, 184-192. https://doi.org/10.1016/j.electacta.2015.02.215.

Tafur, J.P., Santos, F. and Fernández Romero, A.J. (2015), "Influence of the ionic liquid type on the gel polymer electrolytes properties", *Membranes*, **5**(4), 752-771. https://doi.org/10.3390/membranes 5040752.

Tey, J.P, Careem, M.A., Yarmo, M.A. and Arof, A.K. (2016), "Durian shell-based activated carbon electrode for EDLCs", *Ionics*, **22**(7), 1209-1216. https://doi.org/110.1007/s11581-016-1640-2.

Voigt, N. and Van Wüllen, L. (2012), "The mechanism of ionic transport in PAN-based solid polymer electrolytes", *Solid State Ionics*, **208**, 8-16. https://doi.org/10.1016/j.ssi.2011.11.031.

Wang, W., Guo, S., Penchev, M., Ruiz, I., Bozhilov, K.N., Yan, D., Ozkan, M. and Ozkan, C.S. (2013), "Three dimensional few layer graphene and carbon nanotube foam architectures for high fidelity supercapacitors", *Nano Energy*, **2**(2), 294-303. https://doi.org/10.1016/j.nanoen.2012.10.001.

CC